Utilization of Digital Surface Model in Urban Area for Wind Engineering

by

Yasuo Okuda[1], Hisashi Okada[1], Kikitsu Hitomitsu[1], Takaaki Kono[1],
Tetsuro Tamura[2], Shuyang Cao[2], Masamiki Ohashi[3],
Takahisa Kobayashi[4], Osamu Suzuki[4], Hiroshi Yamauchi[4] and Naoki Shirai[5]

ABSTRACT

This paper discusses utilization of digital surface model in urban area for wind engineering; for example, estimation of wind profiles in urban area, estimation of wind loads of tall buildings, and so on. Recent advancement for quality of digital surface model makes it possible to construct sophisticated numerical models for wind flows over roughened ground in urban areas. Urban areas are modeled mainly by the arrangement of buildings with actual shape on the ground surface. LES is carried out for different types of actual urban areas. The validity of the simulated results on wind profiles or wind pressure coefficients and greenery volume in urban area are also discussed.

Key Words: Digital Surface Model, Large Eddy Simulation, Urban Area, Wind Profile,

1. INTRODUCTION

It is very difficult to categorize the wind profile on building site for wind-resistant structural design according to the arrangement of surrounding buildings, houses and plants on the ground. However, there are several recommendations to indicate vertical distributions of mean and fluctuating wind velocities with regard to the surface roughness. These recommendations have been reflected in various international standards and codes, but their definition tends to be ambiguous by showing photos of several roughness examples and so on. Based on this background, we have the aims to deal with the characteristics of urban strong wind on the basis of numerical simulations. Large eddy simulation (LES) is carried out for the estimation of wind profile in the urban area. As for the information on the characteristics of the roughness terrain, we utilize digital surface model. Resent advancement for the quality of Digital surface model makes it possible to construct a sophisticated numerical model for the wind flow over urban areas by using the altitude data for ground surface with fine horizontal resolutions (ex. 2m). With these digital data, the urban area can be represented by the arrangement of buildings with almost actual shape on the ground surface.

In this paper, the validity of the simulation mentioned above is highlighted. First, we show the accuracy of the LES prediction through the comparison with the field measurement data, taking a center of Tokyo and a residential area as the examples of the urban area. Second, we analyze the wind loads on actual high-rise buildings in Tokyo metropolitan sub-center, considering physical mechanism of the behavior of the method of extracting greenery data in Tsukuba area are outlined, which is supposed to be regarded the separated shear

1 Building Research Institute
2 Tokyo Institute of Technology
3 National Institute of Land, Infrastructure and Management
4 Meteorological Research Institute
5 Kokusai Kougyo Co.

layer and the vortices in the wake. And third, the field measurement of wind profile and as the inlet conditions for the LES simulation. These studies are considered to contribute to development of "Numerical Simulator of Urban Wind".

2. ESTIMATION OF WIND PROFILE IN URBAN AREAS

In this section, the results of the LES computations of the boundary layer on the actual urban areas with digital surface model are shown in Figure 1 and its validity is discussed.

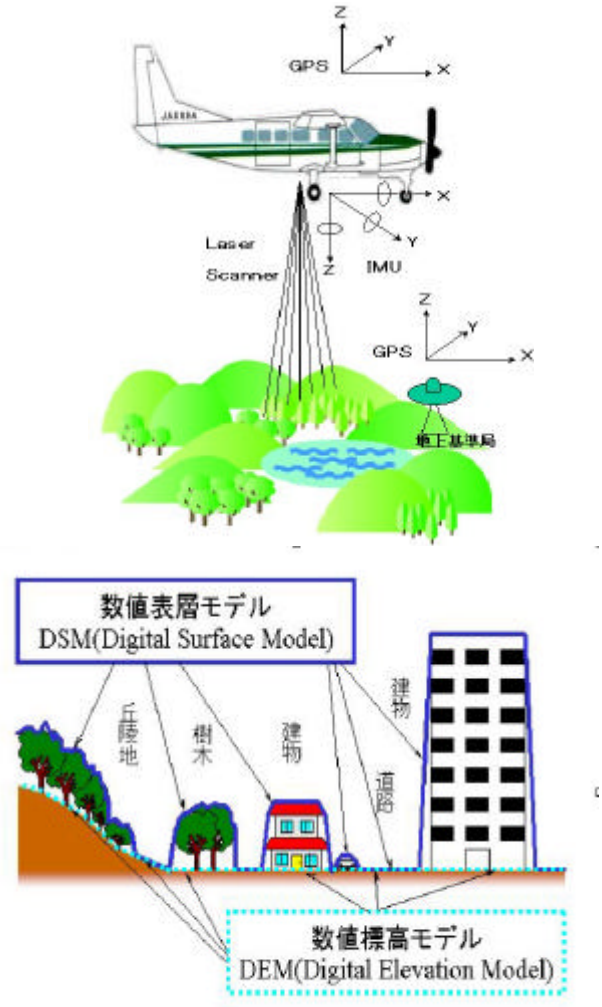

Figure 1 Digital surface model

2.1 Computed Wind Flows in Urban Areas

Figure 2 illustrates two types of urban areas, a center of Tokyo and the residential area. The surface geometries are visualized by digital surface model (RAMS-e, Kokusai Kougyo Co.)[1], whose resolution is potentially 2m, but represented here by 8m grid data. Even by this resolution, we can recognize that there are tall buildings densely arranged in central area, and that in residential area, a-few-storied houses or trees occupy but higher buildings are limited only along the main streets. The computational domain is 2048m in the stream-wise direction, 1024m in the transverse direction and 800m in the vertical direction. For the grid size for computation, 4m is given horizontally as a half of resolution for the surface geometry because of programming efficiency, and 4m is also given vertically in the limited region near the ground and stretched at higher region. As a result, the number of grid is 512 x 256 x 96. The wind direction for computation is given as left to right (south wind).

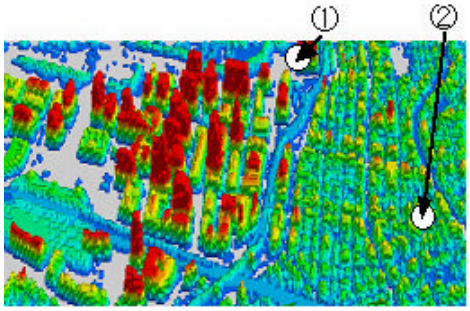

(a) Central area with densely arranged tall buildings

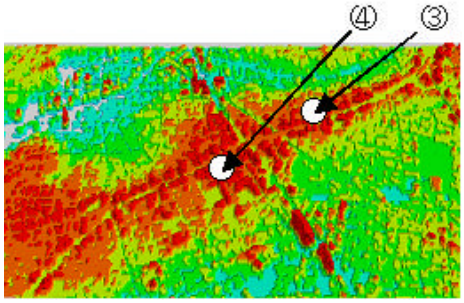

(b) Residential area

Figure 2 Numerical model visualized by digital surface model for urban area of Tokyo

Figure 3 shows the LES results of wind flows in the central area by instantaneous wind velocity contours. The complex structures of wind turbulence with various scales can be seen by contours of the instantaneous velocities close to the ground. It is recognized that the wind flow converges into the street canyon and there is a high wind speed region along the main street or the railway.

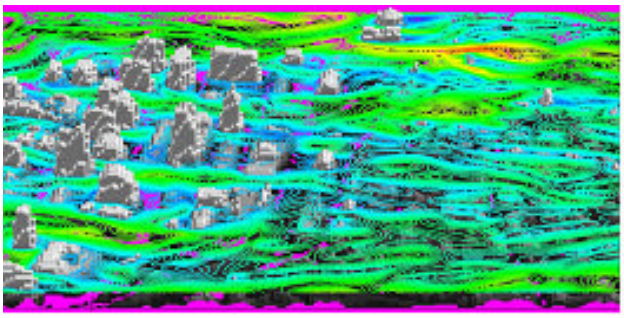

Figure 3 Near-ground instantaneous wind velocity contours in urban area

2.2 Comparison of Simulation Results with Observation Data during Typhoon

The typhoon attacked Tokyo area on September, 11, 2001. The record of wind velocity near ground was gathered at Points ①-④ in Figure 2. We also obtain the wind velocity vectors by analyzing the Doppler radar data at two locations in Kanto area, Narita International Airport and Haneda National Airport. Figure 4 shows the typhoon track represented by the wind velocity vectors. The movement of a typhoon eye is clearly recognized. Figure 5 shows the hourly time variations of the wind velocities and directions for observation data by anemometers and Doppler radars. As the typhoon was approaching and leaving, the velocity magnitude and the wind direction were reasonably changing. Figure 6 shows the comparison between wind profiles computed by LES and observation data. Both data show good agreement with each other.

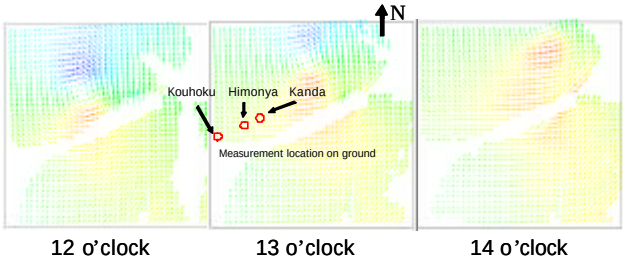

Figure 4 Time variation of wind velocity vectors measured by Doppler radar

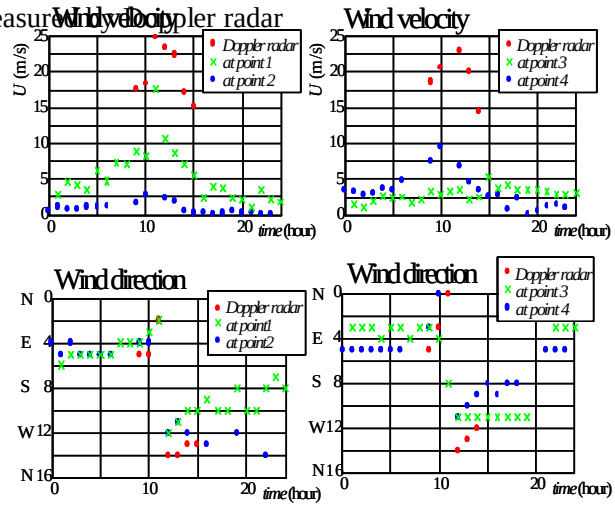

Figure 5 Observation data during Typhoon

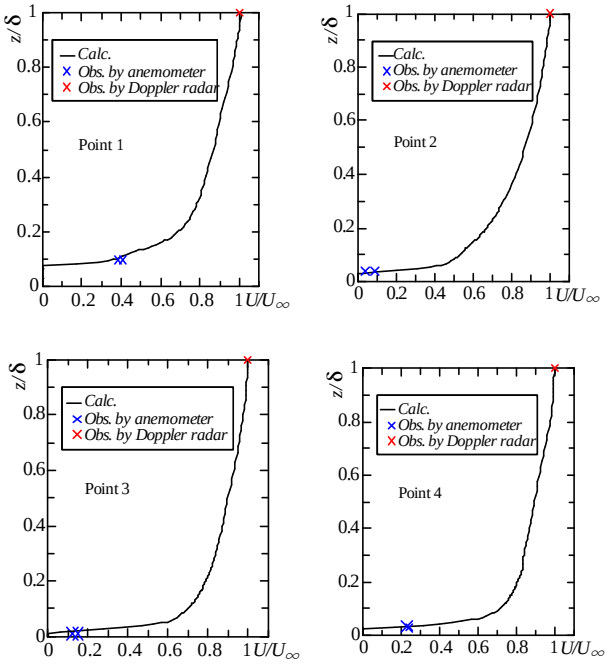

Figure 6 Comparison of simulation results with observation data

2.3 Estimation of Wind Profiles in Urban Areas

In this section, we examine detailed characteristics of the wind profiles in urban areas. Figure 7 shows vertical distribution of roughness parameters, the roughness density and the probability density function of building heights, estimated by Digital surface model. The reasonable results are obtained for both areas. The central urban area has a much higher value for vertical integral l of roughness density than the residential area, but their maximum values for vertical profiles occur almost at same height very close to the ground. By using these roughness parameters, we can estimate the power law exponents of wind profiles based on the empirical rules by Raupach[2] and Counihan[3] (Table 1). For use of Raupach's curve of l vs. z_0/h (z_0: roughness length), the roughness height h is determined by the mean value for the probability density function of building heights. The schematic for estimation procedure of the power law exponent is given in Figure 8. Also, we show the computed wind profiles by LES and the power law exponents estimated by these wind profiles in two types of urban areas (Figure 9). The power law exponents estimated by the empirical procedure, are 0.23 for the central area and 0.21 for the residential area, while 0.27 and 0.19 by wind profiles in the LES results. These differently estimated power law exponents are reasonably coincident with each other in the residential area. But in the central urban area the empirical estimation indicates a small value.

Table.1 Power law exponents of wind profile estimated by roughness parameters

	Central area	Residential area
Roughness density	0.305	0.111
Roughness height (m)	15.22	4.578
Raupach's Z_0 /h	0.053	0.089
Z_0	0.807	0.407
α	0.231	0.205

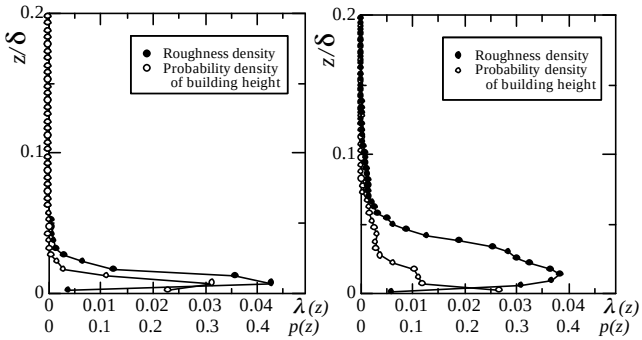

Figure 7 Vertical distributions of roughness parameters estimated by digital surface model

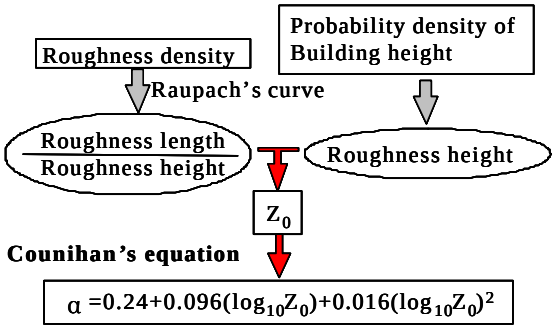

Figure 8 Schematic for estimation procedure of power law exponent

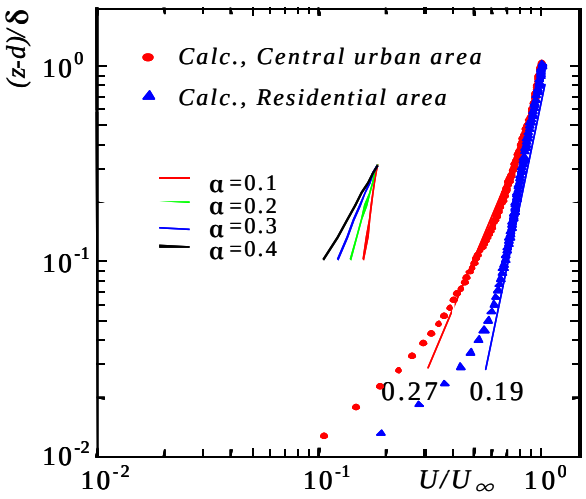

Figure 9 Power law exponents estimated by the wind profiles

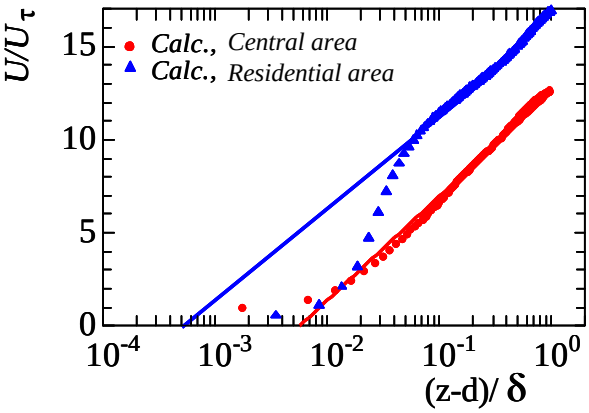

Figure 10 Computed velocity profiles fitted to the log law curves

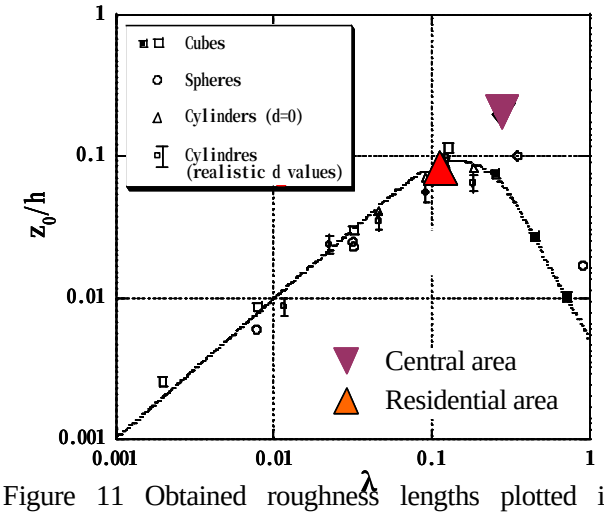

Figure 11 Obtained roughness lengths plotted in Raupach's curve

Next we try to obtain the roughness length z_0 by using the LES results. Figure 10 shows that the computed velocity profiles are fitted to the log law curves. The zero displacement d is determined based on the vertical profile of the computed Reynolds shear stress by Jackson's method[]. The obtained roughness lengths are plotted in the Raupach's figure (Figure 11). The data in the residential area are much coincident, but the computed data in the central area of the city is larger than the Raupach's curve. It causes that roughness length of blocks with various heights does not change to a decrease even as the roughness density much increases, while uniform roughness returns to a smooth-like state. Or, it can be considered as one of the reasons that the height of tall buildings is too high compared to the depth of the turbulent boundary layer, so the universality of roughness parameters comes un-appropriate.

3. ESTIMATION OF WIND LOADS ON TALL BUILDINGS IN URAN AREA

The objective of this section is to analyze the wind loads on actual tall buildings under limit grid resolution, considering physical mechanism of the behavior of the separated shear layer and the vortices in the wake. In this numerical simulation, Immersed Boundary Method, which uses boundary body forces that impose the boundary conditions on a given surface not coinciding with the computational grid, is utilized to reproduce the configuration of the given buildings.

3.1 Computational Model for Tall Buildings at Shinjuku Area

In order to get computational model for actual tall buildings in the urban area, we utilize data of the electronic mapping information at Shinjuku in Tokyo where tall buildings are densely built. The digital surface model represents the ground surface by height of surface roughness (RAMS-e, Kokusai Kogyo Co.) such as buildings and trees. Expression of surface shapes has a resolution of 2m in the horizontal directions. Figure 12 illustrates the perspective view of Shinjuku area with tall buildings, which is visualized by using digital surface model data. Discretization of the area is fine enough to represent the shape of each building or house. The data can be directly transferred to formulate the computational model represented by the Cartesian coordinates for simulating wind flows around actual tall buildings. First we carry out the LES computation for three tall buildings which are selected partly from buildings in Shinjuku area and closely placed with various wall-surface directions (Figure 12). The heights of these three buildings are

more than 200m: building (A) is 209m, (B) is 200m and (C) is 223m. At the present stage of LES computation, we only impose the uniform flow on inflow boundary. But at the next stage, we are planning to simulate the wind flow around tall buildings under the condition that the oncoming flow is set up in the spatially developed turbulent boundary layer.

In this analysis, north wind is assumed as inflow direction. The Reynolds number, based on the uniform flow at the inlet boundary, U, and the real scale length of 50m, L, is 1000. The computational domain is 18L in the stream-wise direction (x) and 20L in the lateral direction (y). 10L is given in the vertical direction (z) to 4.46L of the highest building (C). Three buildings are located at the center in width of the computational domain and 5L distant from the inflow boundary. A non-uniform Cartesian mesh is used and the total number of grid points is 274×268×234. Especially, 168×112×200 grid points are placed to form uniform resolution, L/40, in the vicinity of buildings, while the mesh size is increased with a distance from the buildings. For the boundary condition, free-slip condition is given at the side and top surfaces. No-slip condition is given at the bottom. The outflow boundary is convective outflow condition.

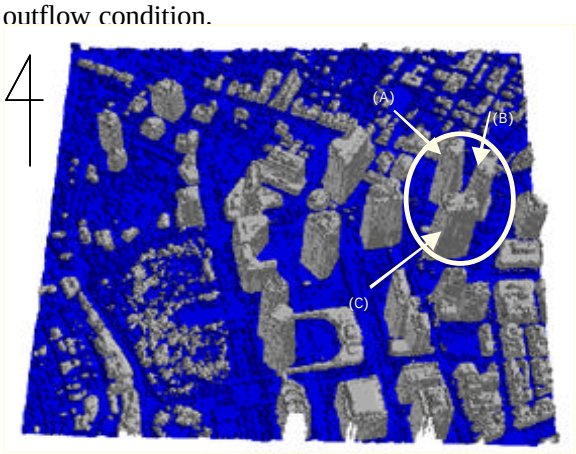

Figure 12 Buildings under consideration in Shinjuku area

3.2 Computed Wind Flow and Aerodynamic Characteristics of Tall Buildings

Figure 13 shows the instantaneous vorticity contours around three tall buildings. We can certainly recognize the vortex structures which are much deformed in the complicated arrangement of these tall buildings. It can be presumed that the wind flow, is coming between two upstream tall buildings, increases its velocity and impinges on the frontal surface of a downstream tall building. Also, strong horse shoe vortex can be seen at the bottom of the tall building in Figure 13(a). According to details of flow patterns in Figure 13(b), the separated shear layer from the upper corner of building (A) comes close to the building (A), affected by the wall of building (B). The wake flows of building (A) cover the frontal region of building (C).

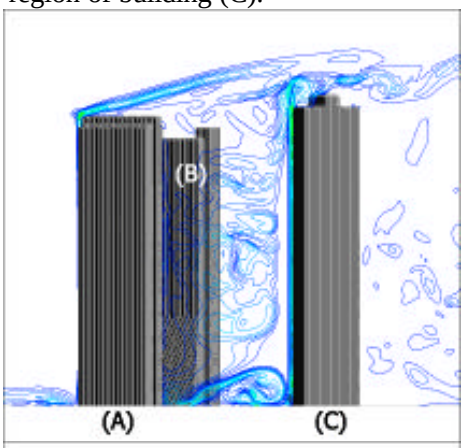

(a) x-z plane

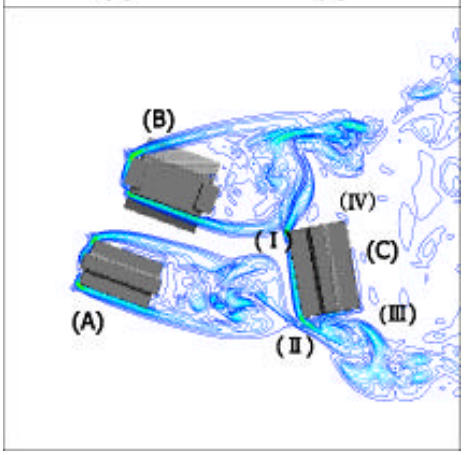

(b) x-y plane

Figure 13 Instantaneous vorticity contours around three tall buildings

As a result, the pressure distribution on the frontal surface of building (C) is largely deformed, as seen in Figure 14(a). In Figure 14(b) we also recognize an interaction of shear layers separated from lower corner of building (B) and upper corner of (C). Because the vorticity of these shear layers has an opposite sign, the vortices of the shear layers are made weaken each other, and eventually the shear layer of building (C) keeps away from the wall. The pressure distribution on the surface (Ⅳ)-(Ⅰ) of building (C), shown in Figure 14, indicates the slight recovery. Figure 14(b), also, shows that turbulence in the wake region of building (A) affects behavior of the lower shear layer from building (C). The shear layer increases the occurrence to reattach to the after-body of building (C), and the pressure distribution displays a slight reduction of C_p on the surface (Ⅱ)-(Ⅲ), in Figure 14. A strong horse shoe vortex at the bottom of the building (C) shown in Figure 13(b) has a much influence on surrounding wind environment. Wind load is also influenced by the adjacent buildings and the frontal pressure in lower region decreases compared to the case of a single building.

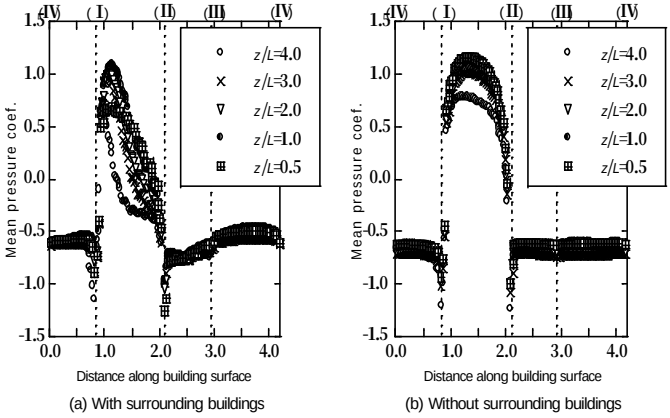

Figure 14 Time averaged wind pressure coefficient along the surface of the building (C)

4. ESTIMATION OF WIND PROFILE AND GREENERY VOLUME IN URBAN AREA

In this section, the field measurement of wind profile and the method of extracting greenery data in Tsukuba area are outlined. As for the field measurement, wind profiles are measuring at two different points, which makes it possible to evaluate the special structure of strong wind in the given region. And by the evaluation of the greenery volume, we can numerically discuss the degree of effect of trees on the urban roughness condition. Such information is applied in the numerical simulation on the wind environment in Tsukuba area.

4.1 Comparison of Characteristics on Wind Profiles in Tsukuba Area

Authors have carried out the wind field measurement in Tsukuba area, where is supposed to be flat field with rare topographic ups and downs. As shown in Figure 15, Doppler Sodar installed in Building Research Institute (BRI) and super sonic anemometers at an observation tower, 213m high, in Meteorological Research Institute (MRI) are used for the wind measurement. MRI is located about 10km to the south from BRI. In this section, measurement results on March 3rd through 21st are outlined.

As for the wind velocity and direction between two places, it is confirmed that there is a certain correlation as shown in Figure 16. On the vertical profile of the wind velocity, averaged index of the power law in MRI is larger than that in BRI and depends on wind velocity as shown in Figure 17. The averaged values in MRI are 0.40 against northern wind and 0.33 against western wind, while those in BRI are 0.19 against northern wind and 0.21 against western wind, respectively. As for the index in MRI, the averaged index from northern wind is larger than that from western wind, which is probably because there is an urban area with middle-rise buildings to the north of MRI, where there is relatively rural distinct to the western of MRI. Cross-correlation coefficients obtained from every ten minutes' index of the power law of the each point are shown in Figure 18. They

result in getting maximum values at time lag of 10 through 20minutes, which means that it is useful to evaluate the profiles by considering wind with time scale of a few ten minutes. One example of the each profile is in Figure19.

(a)Monostatic Doppler Sodar (BRI)

(b)Obseravation tower (MRI) with anemometers

Figure 15 Wind measument systems

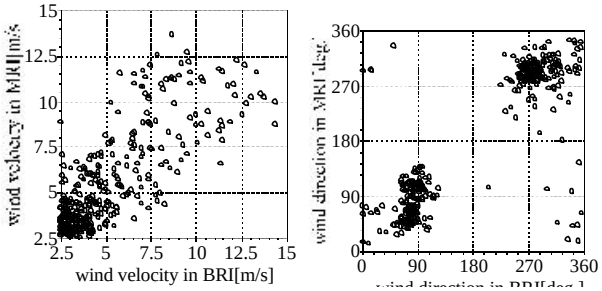

Figure16 10-min averaged wind velocity and direction by the Monostatic Doppler Sdar in BRI and super sonic anemometer in MRI

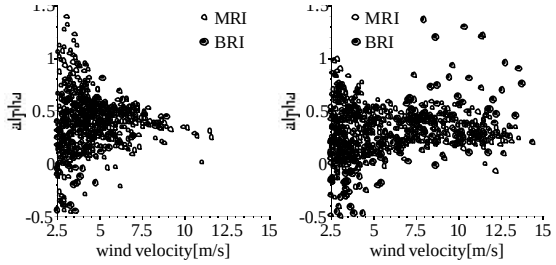

(a) NW– NE (b) SW – NW

Figure 17 Wind velocity and index of power law

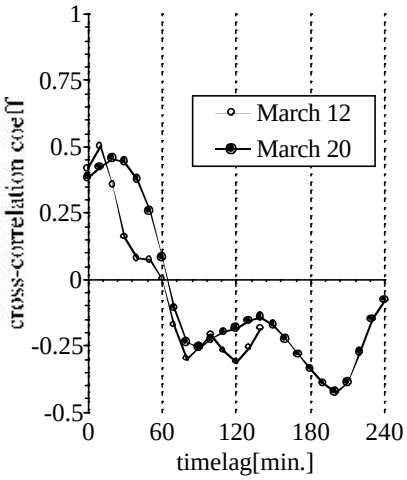

Figure 18 Cross-correlation coefficients of power law index in BRI and MRI

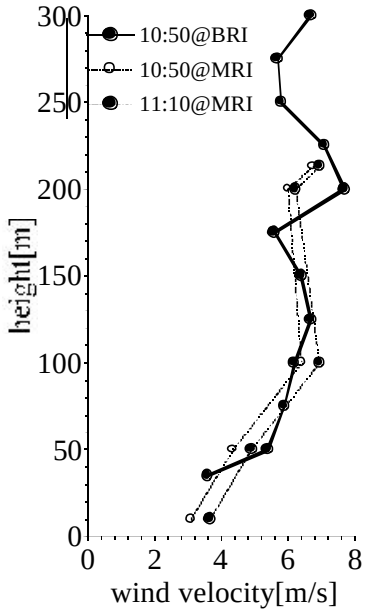

Fig.19 Example of wind profile in BRI and MRI at 10:50 and 11:10 on March 20th

4.2 Numerical Evaluation of Greenery Volume in Tsukuba Area

We use IKONOS satellite images superposed on digital surface model data in order to extract greenery volume in some urban areas. However, in this section we introduce another scheme of using only digital surface model data to analyze urban greenery coverage. Figure 20 shows small target region of

Tsukuba area, field size is 180m x 180m. The ground surface measure result of this place by airborne LIDAR is shown in Figure 21 as a same direction view of Figure 20, and top view of this region is shown in Figure 22. It shows the canopy of trees has a characteristic geometric pattern like a hedgehog. We extracted the greenery coverage area from digital surface model data using this feature. We have chosen Co-occurrence Matrix [4] for method of this study, on the analogy of image analysis. Co-occurrence Matrix can be obtains complexity information of target region. If accumulate concentrate to the near diagonal lines of this matrix then it meaning flat surface pattern like a building top else if distributed separate from the diagonal line then it have a complex pattern like a canopy of tree. Parameterized this matrix pattern used for extracting greenery coverage. The calculation parameters of Co-occurrence Matrix, displacement vector is d=1 used at all four directions (q=0, 45, 90, 135 $^\circ$) and the number of height levels is L=10 (ground level to 50m height divided into 10 levels). The examine window size is 3 x 3 at each point. The results of the calculation are shown in Figure 23.

These results suggest will be useful to making it possible to calculating the greenery volume in urban area by digital surface model made from only airborne LIDAR data.

Figure 20 Target region (180m x 180m)

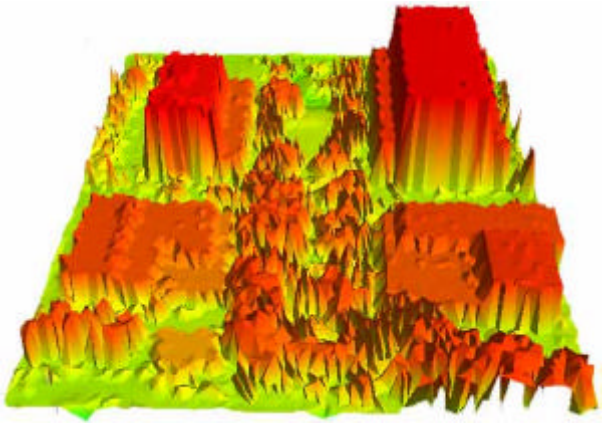

Figure 21 Digital surface model made by airborne LIDAR shown by TIN (Triangulated Irregular Network)

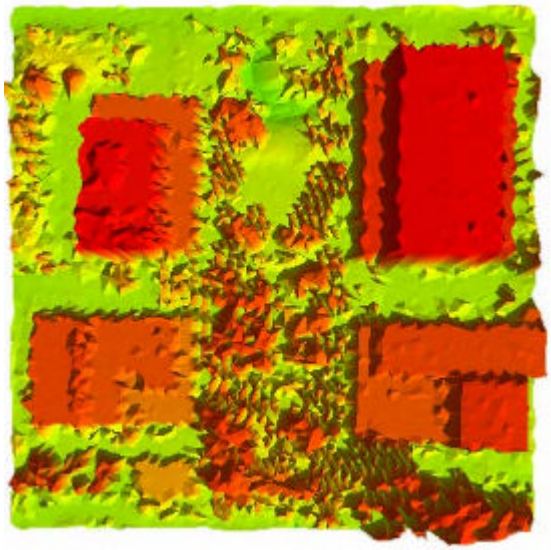

Figure 22 Top view (TIN)

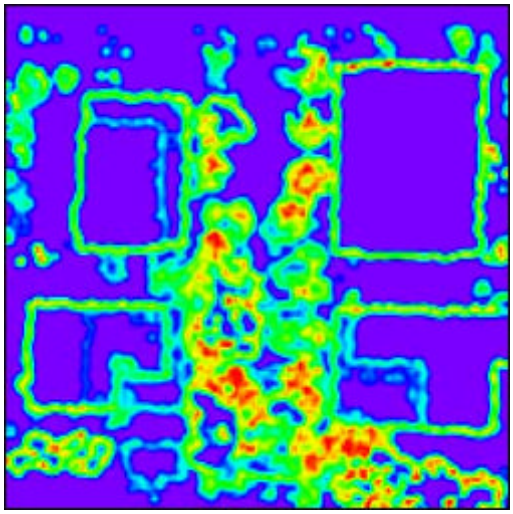

Figure 23 Greenery extractions(q=0+45+90+135 $^\circ$)

3. CONCLUSIONS

In this paper, the evaluation of urban wind characteristics by numerical methods was introduced and their validity was discussed. The fundamental techniques in this paper will work for developing of "Numerical Simulator of Urban Wind".

REFERENCES

[1] Okuda Y., Okada H., Tamura T. et al., *Use of Digital Surface Model for Estimation of Surface Roughness in Urban Area*, Proc. of 17th National Symposium on Wind Engineering, pp.13-18, 2002.

[2] Raupach M.R. Antonia R.A. and Rajagopalan S. , *Rough-wall turbulent boundary layers*, Appl. Mech. Rev., Vol. 44, pp.1-25, 1991.

[3] Counihan, J., *Adiabatic Atmospheric Boundary Layers*, Atmos. Environ., Vol. 9, pp. 871-905, 1975.

[4] Haralick R. M., *Statistical and structural approaches to texture*, Proc. IEEE, Vol. 67, No. 5, pp. 786-803, 1979.